NUCL SCI TECH (2016) 27:2
DOI 10.1007/s41365-016-0007-8

Simulation of storage ring injection of HLS II

Yuan-Yuan Wang[1] · Lei Shang[1] · Feng-Lei Shang[1] · Ye-Ming Lu[1]

Received: 9 February 2015 / Revised: 1 April 2015 / Accepted: 9 April 2015 / Published online: 27 February 2016

Abstract The Hefei light source (HLS) has been upgraded into HLS II, with increased brightness and stability. In this paper, the new injection system is described. Elegant program is used to simulate the particles motion in 6D phase space. In the process of tracking simulation of electrons, the system tolerances and magnet errors are introduced. Influences to the injection efficiency from beam injection deviation are studied. These provide important reference for realizing the Top-up injection.

Keywords Injection system · Bump orbit · Injection simulation · Beam deviation · Injection efficiency

1 Introduction

Hefei light source, of 800 MeV electron beam energy, has been upgraded into HLS II [1] with increased number of straight sections (from four to eight) by changing the magnet focusing structure of the storage ring, of the same circumference as before. The aim is to install more insertion devices and improve brightness of the light source. The main specifications of HLS II are listed in Table 1. Where, ε_x is the horizontal emittance, v_x/v_y is the betatron tune, $\xi_x N/\xi_y N$ is the natural chromaticity, α is the momentum compaction, τ is the damping time, J is the damping partition number, σ_δ is the energy spread and β_{xy} is the beta-function.

✉ Lei Shang
lshang@ustc.edu.cn

1 National Synchrotron Radiation Laboratory, University of Science and Technology of China, Hefei 230029, China

For future development of the Top-up mode, a major transformation of the injection system of storage ring was done. According to characteristics of HLS, the distributed four-kicker bump orbit scheme was adopted [2–5]. This scheme can reduce the kicker strength and improve flexibility of adjusting the shape of bump orbit. Figure 1 shows a layout of the new injection bump orbit system.

Considering beam orbit distortion, beam size and other factors, the height of orbit bump is 24 mm and the septum inside is 29 mm from the equilibrium orbit. To have a good field region, the electron beams are injected at 2 mm away from the septum outside and 33 mm to equilibrium orbit. The horizontal aperture of vacuum chamber is 22 % smaller than that of the HLS before upgrading. This reduces the demand for magnet aperture. Figure 2 shows the horizontal phase space of injection system at injection point.

In order to achieve the required height of bump orbit, we need to calculate the deflection angles of four kickers. According to the conditional expression of four-kicker bump orbit [6] with zero angle at injection point:

$$\theta_1 = [b/(\beta_0\beta_1)](\cos\Delta\Psi_{02} - \alpha_0 \sin\Delta\Psi_{02})/\sin\Delta\Psi_{01}, \quad (1)$$

$$\theta_2 = [b/(\beta_0\beta_2)](\cos\Delta\Psi_{01} - \alpha_0 \sin\Delta\Psi_{01})/\sin\Delta\Psi_{21}, \quad (2)$$

$$\theta_3 = [b/(\beta_0\beta_3)](\cos\Delta\Psi_{40} - \alpha_0 \sin\Delta\Psi_{40})/\sin\Delta\Psi_{43}, \quad (3)$$

$$\theta_4 = [b/(\beta_0\beta_4)](\cos\Delta\Psi_{40} - \alpha_0 \sin\Delta\Psi_{30})/\sin\Delta\Psi_{43}, \quad (4)$$

where α and β are the twiss parameters in the horizontal direction, $\Delta\Psi_{ij}$ is the phase-advance from Ψ_i to Ψ_j, and b is height of the bump orbit. Deflection angles (in mrad) of the four injection kickers (K1–K4) are 6.4825, 3.4583, 3.4583 and 6.4825, respectively, calculated at the design height of bump orbit with the orbit angle being zero at injection point. Figure 3 shows the shape of local bump orbit.

Table 1 Main specifications of HLS II

Specifications	Values
ε_x (nm rad)	37.14
ν_x/ν_y	4.445/2.316
$\xi_x N/\xi_y N$	−7.42/−7.43
α	0.0158
$\tau_x/\tau_y/\tau_s$ (ms)	19.5/21.0/10.9
$J_x/J_y/J_s$	1.076/1/1.924
σ_δ	0.00047
$\beta_{xy\|\max}$	19.49/14.78
$\beta_{xy\|\min}$	1.81/1.61
$\beta_{xy\|\mathrm{ave}}$	6.26/5.82
$\eta_{x\|\max}$	1.22

Table 2 Errors (in 3σ) of storage ring included in the simulations

Error source	Value
Quadrupole alignment $\Delta x/\Delta y/\Delta z$ (mm)	0.08/0.08/0.50
Quadrupole rotation $\Delta\Phi$ (mrad)	0.20
Sextupole alignment $\Delta x/\Delta y/\Delta z$ (mm)	0.08/0.08/0.50
Sextupole rotation $\Delta\Phi$ (mrad)	0.20
Kicker alignment $\Delta x/\Delta y/\Delta z$ (mm)	0.20/0.20/0.20
Kicker rotation $\Delta\Phi$ (mrad)	0.5
Kicker field time jitter (ns)	2.0
Kicker field amplitude jitter (%)	0.15

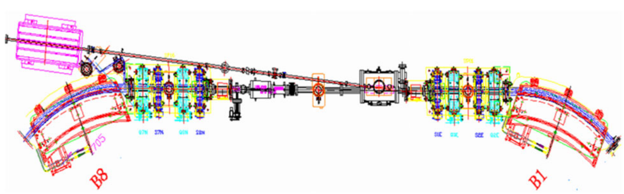

Fig. 1 (Color online) Layout of the new injection bump orbit system

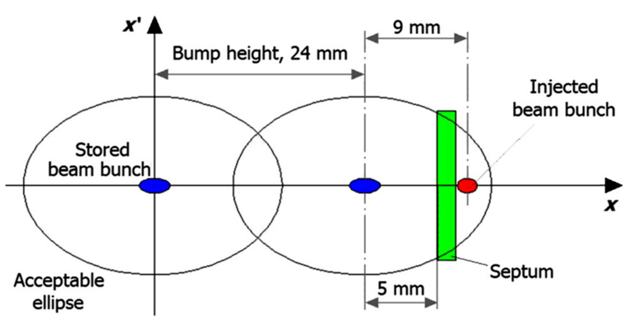

Fig. 2 (Color online) The horizontal phase space at the injection point

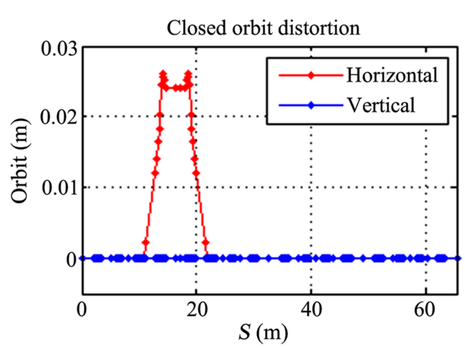

Fig. 3 The shape of local bump orbit

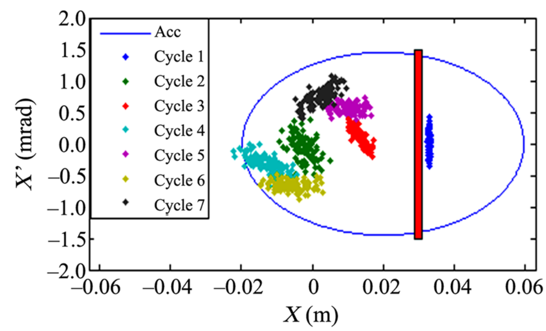

Fig. 4 (Color online) Particles tracking for an injected beam in the horizontal phase space

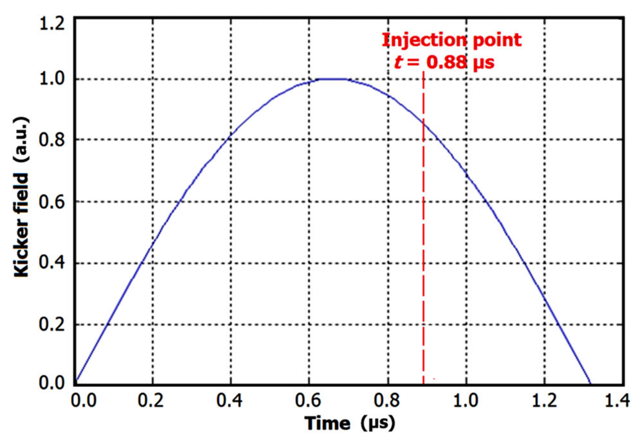

Fig. 5 (Color online) The waveform of kicker field and the injection time point

The septum thickness is 2 mm, due to limitation of the pulse septum technology. Considering orbit distortion and size of the injected beam, the ideal launching condition for an injected beam center in 6D phase space is set to $(x, x', y, y', s, \delta) = (33\,\mathrm{mm}, 0, 0, 0, 0, 0)$. A multiparticle beam of Gaussian distribution is used for tracking simulations of injection process [7, 8]. Various system and project errors are included to obtain realistic simulations of injection process.

2 Injection simulation

The simulations using Elegant were carried out [9, 10]. Through analysis of numerical simulation results, performance of the new injection system could be determined. Practically, alignment and rotation errors of the magnets were considered in the simulation. And, errors of the new injection system, such as amplitude jitter, time jitter, alignment and rotation errors, etc. (Table 2), were considered, too. For all the errors, a multiparticle beam of Gaussian distribution is used for tracking simulations of the injection process. Figure 4 shows the first seven turns of particles tracking for an injected beam in the horizontal phase space.

The waveform of kicker field is a half-sine wave and pulse width is 1.32 µs. The injection time is selected on the falling edge of half-sine wave at 0.88 µs relative to the initial time. Figure 5 shows the waveform of kicker field and the injection time point. It is obvious that the bump orbit shrinks faster. The HLS storage ring is 66.13 m in circumference, with a beam bunch cycling period of 0.22 µs [6, 11]. The orbit bump shall disappear completely after running 2 cycles. Table 3 lists the main parameters of the kickers and pulse septum.

The oscillation amplitude [12] in vertical direction is derived from the vertical injection angle and position deviation of the injected beam. The rotating angle errors of kickers and the transverse coupling caused by rotation errors of other components are also important influence

Table 3 Main parameters of the kickers and pulse septum

Parameters	Kickers	Pulse septum
Maximum injection energy	1 GeV	1 GeV
Maximum deflection angle	8 mrad	105 mrad
Integral field	0.027 Tm	0.35 Tm
Peak field strength	1050 G	8750 G
Yoke physical length	200 mm	400 mm
Aperture size	80 mm × 54 mm	10 mm
Magnetic inductance	0.47 µH	4.2 µH
Excitation current peak	4514 A	5570 A
Half-sine width	1350 ns	60 µs

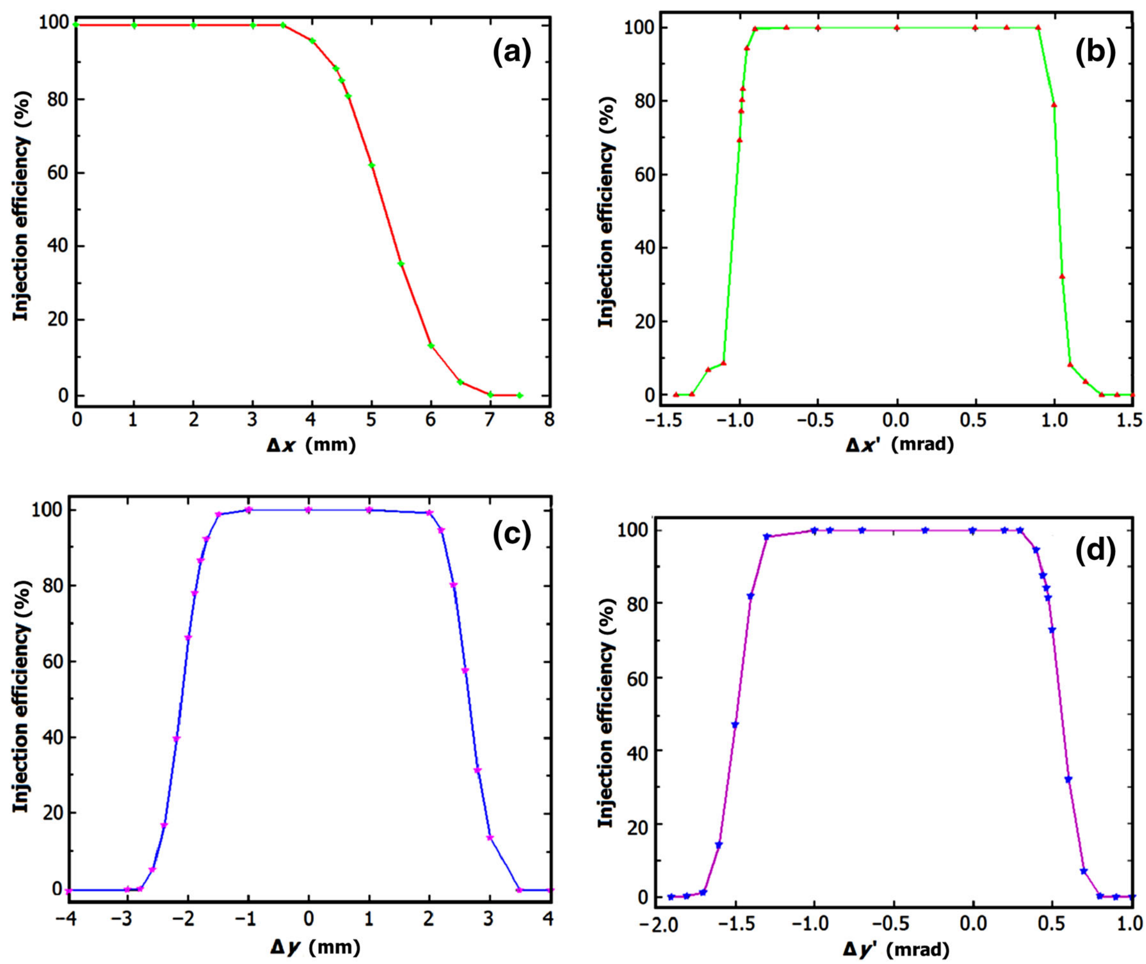

Fig. 6 (Color online) The injection efficiency under four types of injection deviation

factors. Compared with the horizontal oscillation amplitude, the vertical beam emittance caused by these errors is far less than those caused by the ring vertical aperture.

We used 1000 electrons to represent an injected beam bunch. From the moment of injection starting, we tracked the electrons for 1000 cycles and determined the injection efficiency by observing the number of missing particles. The initial state of an injected beam depends on parameters at the end of transfer line. The twiss parameters at the end of transport line are $\beta_x = 7.917$ m, $\beta_y = 5.718$ m, $\alpha_x = 0.067$, $\alpha_y = -0.725$, $\varepsilon_x = \varepsilon_y = 25.56$ nmrad, and $\sigma_\varepsilon = 0.0048$. Errors of the existence of transport line and injection system cause variations in launching condition of transverse phase space for an injected beam. We, respectively, scanned the initial value of injected beam on x, x', y, and y' directions, and checked the beam capture efficiency. Figure 6 shows the injection efficiency under the condition of four types of injection deviation. Deviation ranges of the injected beam to ideal condition are $\Delta x(\mathrm{mm}) = [0.0, 4.6]$, $\Delta x'(\mathrm{mrad}) = [-0.985, 0.99]$, $\Delta y(\mathrm{mm}) = [-1.87, 2.4]$, and $\Delta y'(\mathrm{mrad}) = [-1.4, 0.4]$, when the injection efficiency is above 80 %.

3 Conclusion

The Top-up mode injection of HLS II requires high injection efficiency and beam stability of the injection system. Through numerical simulation for the injection process of the new injection system, we determined the tolerance of errors. This provides an important reference for improving the injection efficiency and stability of HLS II. Later, high injection efficiency can be achieved by adjusting the parameters of transport line and septum according to the results. So it can be a steppingstone for the commissioning and operation of Top-up in the future.

Acknowledgments Supported by National Natural Science Foundation of China (No. 11175181).

References

1. I. Hwang, J.Y. Huang, M. Kim et al., Top-up operation at Pohang Light Source-II. Rev. Sci. Instrum. **85**, 055113 (2014). doi:10.1063/1.4878256
2. E.D. Van Garderen, K.R. Bambery, M. Clift et al., Instrumentation upgrade for Top-Up operations at the Australian Synchrotron. J. Phys. Conf. Ser. **425**, 042015 (2013). doi:10.1088/1742-6596/425/4/042015
3. M. Adachi, H. Zen, T. Konomi et al., Design and construction of UVSOR-III. J. Phys. Conf. Ser. **425**, 042013 (2013). doi:10.1088/1742-6596/425/4/042013
4. W. Lin, L. Weimin, Y.F. Guang et al., The upgrade project of Hefei light source (HLS). Proceedings of the IPAC 10, Kyto, Japan, 2010, pp. 2588–2590
5. L. Wang, W.M. Li, Y.F. Guang et al., Physical design of full energy injection system in HLS. J. Univ. Sci. Technol. China (2007), Z1
6. X.Q. Wang, L. Shang, L. Wang et al., Research and development for injection system of HLS storage ring in NSRL Phase II Project. J. Univ. Sci. Technol. China **37**, 4–5 (2007)
7. K.J. Fan, G.Y. Feng, X.Q. Wang et al., Feasibility study of full energy injection of HLS injection bump system. High Power Laser Part. Beams **12**, 624–628 (2000)
8. X.Q. Wang, Y.J. Pei, L. Shang et al., The progress of development of four kickers bump system for injection in HLS ring. IEEE Part. Accel. Conf. **2**, 1315–1317 (1999)
9. C.C. Chiang, P.J. Chou, Injection simulations for TPS storage ring. Proceedings of IPAC2013 (MOPWO058), Shanghai, China, 2013
10. R. Apsimon, B. Balhan, M.J. Barnes et al., Design of the injection and extraction system and related machine protection for the Clic Damping Rings. CERN-OPEN-2014-044, 2014
11. M. Borland, A.N.L. Argonne et al., Features and applications of the program Elegant. Proceedings of IPAC2013, Shanghai, China, 2013
12. M. Borland, elegantRingAnalysis: an interface for high-throughput analysis of storage ring lattices using elegant. IEEE Particle Accelerator Conference, 2005, pp. 4200–4202. doi:10.1109/PAC.2005.1591764
13. K. Amyx, J. Balasalle, J. King et al., Beam dynamics simulations with a GPU- accelerated version of elegant. Proceedings of IPAC2013, Shanghai, China, 2013
14. G.B. Zhao, R.X. Yuan, Z.C. Chen et al., Development of button-type pickup for SSRF ring. Nucl. Sci. Technol. **25**, 060103 (2014). doi:10.13538/j.1001-8042/nst.25.060103
15. B.H. Oh, J. Lee, M. Yoon et al., Beam optics correction in the PLS-II storage ring. J. Korean Phys. Soc. **63**, 1268–1273 (2013). doi:10.3938/jkps.63.1268
16. M. Sjöström, E. Wallén, M. Eriksson et al., Corrector-based magnet alignment procedure. Nucl. Instrum. Methods **597**, 170–177 (2008). doi:10.1016/j.nima.2008.09.011
17. L. Shang, X.Q. Wang, L. Wang et al., New injection kicker modulators for HLS ring. Proceedings of the 2001 Particle Accelerator Conference, Chicago, 2001
18. L. Wang, K.J. Fan, L. Shang et al., Study of pulse magnetic field calculation of kicker magnet in HLS storage ring. Nucl. Technol. **2**, 002 (2003) (**in Chinese**)
19. T. Takayanagi, T. Ueno, K. Horino et al., Comparison of the pulsed power supply systems using the PFN switching capacitor method and the IGBT chopping method for the J-PARC 3-GeV RCS injection system. IEEE Trans. Appl. Supercond. **24**, 1–5 (2014). doi:10.1109/TASC.2013.2294400
20. M. Kim, I. Hwang, S.J. Park et al., Tracking study of transient behaviors at beam injection of the PLS-II ring. J. Korean Phys. Soc. **63**, 2072–2079 (2013). doi:10.3938/jkps.63.2072